Egyptian Journal of Radiology and Nuclear Medicine

RESEARCH

Open Access

T2 mapping post acute myocardial infarction: a novel technique in assessing myocardial edema

Maha Mourad Mohyeldin Elsaid[1*], Basant Mohamed Raief Mosaad[1], Hend Galal Eldeen Mohamed Ali Hassan[1,3], Youssef Mohamed Mohamed Fahmy Amin[2] and Ahmed Samir Ibrahim[1]

Abstract

Objective Cardiovascular magnetic resonance (CMR) is considered the gold standard imaging modality for assessing myocardial infarction lesions, offering precise myocardial tissue characterization. Elevated transverse relaxation time (T2) serves as a specific indicator of increased myocardial water content, thus becoming a valuable index for myocardial edema. However, conventional T2-weighted CMR sequence exhibits several limitations, primarily providing qualitative information. In contrast, recently developed quantitative T2 mapping techniques overcome these limitations, enabling a more reliable assessment of myocardial edema. These techniques offer the advantage of diagnosing and monitoring myocardial injury without the necessity of contrast agents. Our study aims to add to a growing literature demonstrating the efficacy of quantitative T2 mapping technique to detect and quantify regions of myocardial edema post-myocardial infarction.

Result Native T1 and T2 mapping accurately identified myocardial edema in all patients enrolled in the study. Notably, native T1 and T2 values exhibited a significant elevation in the infarcted myocardium compared to the remote myocardium (for T1: 1295.50 ± 87.65 vs. 1074.95 ± 92.86 ms, respectively; and for T2: 74.63 ± 6.51 vs. 52.53 ± 6.26 ms, respectively; $p < 0.0001$ for both). Microvascular obstruction was observed in 12 out of 20 patients, affecting one or more myocardial segments within the infarct areas. Among this subgroup, regions with a microvascular obstruction within the infarct zone displayed lower T1 and T2 values compared to areas of infarction without microvascular obstruction (for T1: 1115.05 ± 64.70 vs. 1295.50 ± 87.65 ms, respectively; and for T2: 53.65 ± 3.56 vs. 74.63 ± 6.51 ms, respectively; $p < 0.0001$ for both). Additionally, we provided reference values for myocardial T1 and T2 specific to our facility's 1.5 Tesla CMR system, applicable to both infarct and remote myocardium.

Conclusion Parametric T1 and T2 mapping techniques can detect and quantify myocardial edema resulting from myocardial infarction. The presence of microvascular obstruction that results from revascularization injury affects both T1 and T2 values. This information can be used and has broad clinical implications for diagnosis and guiding or monitoring the treatment of myocardial infarction.

Keywords Acute myocardial infarction, Cardiac magnetic resonance, T2-weighted imaging, T1/T2 mapping, Microvascular obstruction, 1.5 T

*Correspondence:
Maha Mourad Mohyeldin Elsaid
mahamourad00@gmail.com
Full list of author information is available at the end of the article

Background

Acute myocardial infarction (AMI) is one of the leading causes of mortality and morbidity worldwide [1]. Following AMI, patients' prognosis depends on various factors, including infarct size, percentage of salvaged myocardium post-reperfusion, microvasculature status within the infarct zone, and residual left ventricular (LV) function [2].While early restoration of blood flow to the ischemic myocardium is pivotal in limiting infarct size and reducing the risk of future heart failure and mortality, it paradoxically induces reperfusion injury, marked by microvascular lesions, inflammation, and edema, all of which contribute to adverse left ventricular remodeling and patient outcomes [3–7]. Conventional CMR techniques, including T2-weighted and post contrast T1-weighted sequences, can detect myocardial infarction and edematous areas [8]. However, these techniques offer qualitative rather than quantitative data, limiting their utility in follow-up examinations or comparative analyses among other subjects [9]. Moreover, problems inherent to T2-weighted CMR images such as surface coil intensity variations, high subendocardial signal from stagnant blood, and susceptibility to motion artifacts, have limited its widespread clinical acceptance for detecting myocardial edema [10]. Recent advancements in T1 and T2 parametric mapping techniques have demonstrated the ability to overcome these limitations, providing rapid, reproducible, and gadolinium-free acquisitions [7]. These techniques directly measure T1 and T2 relaxation times of tissues on a pixel-by-pixel basis, reflecting myocardial water content and injury severity [8, 9, 11–14]. Importantly, the values derived from T1 and T2 mapping techniques have prognostic significance through providing quantitative data on tissue characteristics that enable clinicians to assess therapeutic efficacy and tailor management strategies accordingly [11]. Despite their clinical promise, challenges in standardization persist, with mapping methods being site and vendor-specific, thereby hindering their integration into clinical decision-making and multicenter studies [15, 16]. Consequently, the need for establishing local reference values for T1 and T2 mapping specific to each imaging facility is emphasized [16]. Our study aims to evaluate the efficacy of these mapping techniques in detecting myocardial edema post-AMI thereby contributing to improved patient care.

Methods

Study population

The study prospectively enrolled twenty Patients with acute myocardial infarction (AMI), as defined by established diagnostic criteria [17], who presented to the Emergency Department (ED) and treated with primary percutaneous coronary intervention (P-PCI) in the Cardiology Department of Ain Shams University Hospital in the interval between June 2020 and December 2023. Medical history, clinical and electrocardiographic findings, as well as serological markers were recorded at admission. Patients with hemodynamic instability, a history of previous myocardial infarction or cardiomyopathy, as well as those with contraindications to CMR (e.g., non-MRI-compatible cardiac devices, aneurysmal clips, and cochlear implants) or MRI contrast, were excluded from the study. All patients provided written informed consent to participate in this study.

CMR acquisition

CMR imaging was conducted on all patients utilizing a 1.5 T Philips machine (Philips Achieva—XR Medical systems, Best, Netherlands), utilizing a dedicated phased array cardiac receiver coil.

CMR protocol

The CMR imaging protocol included the following sequences: Left ventricular (LV) cine imaging, T2-weighted short tau inversion recovery (T2W STIR), native T1 mapping, T2 mapping, and late gadolinium enhancement (LGE). All short-axis images were aligned with the cine short-axis slice position. T2W STIR, T1 mapping, and T2 mapping sequences were performed before administering gadolinium contrast. These sequences were obtained at basal, mid-ventricular, and apical short-axis levels, and were precisely aligned with the same plane as the short-axis cine images.

Cine imaging

Balanced steady-state free precession (bSSFP) cine images were acquired in both the four-chamber view and a stack of short-axis (SAX) slices covering the ventricles. Imaging parameters were repetition time (TR) of 2.8 ms, echo time (TE) of 1.38 ms, voxel size of 176×133, flip angle (FA) of 60°, field of view (FOV) of 350×286 mm^2, slice thickness of 8 mm, sensitivity encoding (SENSE) factor = 2, and acquisition of 30 cardiac phases.

T2-weighted STIR imaging sequence

Edema-sensitive black-blood T2-weighted magnetic resonance (MR) imaging was conducted on the end-diastolic left ventricular short axes, employing a fat-suppression short tau inversion recovery (STIR) sequence. Imaging parameters were TR of 1600 ms (equivalent to two R-R intervals); TE of 90 ms; voxel size of 1.36×1.36×10 mm^3; and a FA of 90°.

Native T1 mapping

T1 mapping data were acquired using the balanced steady-state free precession (SSFP)-based modified

look-locker inversion recovery (MOLLI) technique [18]. The MOLLI scheme employed was a 3-beat (3s) 5-beat pattern, consisting of three acquisitions after the first inversion pulse, followed by two 3-heartbeat pauses and a third inversion for the last five acquisitions [19, 20]. The imaging parameters were as follows: TR of 2.2 ms, TE of 1.02 ms, voxel size of $2\times2\times10$ mm^3, FA of 35°, FOV of 380×256 mm^2, slice thickness of 10 mm, and SENSE factor = 2.

T2 mapping

T2 mapping data were acquired using a navigator-gated black blood-prepared gradient spin-echo sequence (GraSE) [20]. The imaging parameters were set as follows: TR of 1 heartbeat, 9 echoes, TE of 12 ms, echo spacing (ΔTE) of 6.2 ms, voxel size of $2\times2\times10$ mm^3, FA of 90°, echo planar imaging (EPI) factor of 3, FOV of 380×380 mm^2, slice thickness of 8 mm, and SENSE factor = 2.

Late gadolinium enhancement

LGE imaging was conducted 10 min post-injection of a bolus containing 0.1 mmol/kg of gadoterate meglumine (Dotarem). Utilizing a three-dimensional phase-sensitive inversion-recovery gradient-echo T1 sequence (PSIR) after adjusting the inversion time to nullify normal myocardium. Images were acquired in the same planes as the bSSFP cine images, with the following imaging parameters: TR of 5.50 ms, TE of 2.40 ms, voxel size of $1.36\times1.36\times8$ mm^3, and a flip angle of 15°.

Image analysis

Dedicated software (Philips IntelliSpace Portal workstation, version 8.0) was used for analysis and post-processing. Two experienced cardiac imaging radiologists independently evaluated all images. In the case of disagreement, a third radiologist would be asked to independently evaluate the images to reach a consensus.

Evaluation of left ventricular function

Cine images in the short-axis (SAX), 2-chamber and 4-chamber views were assessed for wall motion abnormalities. Left ventricular ejection fraction (LVEF) was automatically calculated after manually contouring the epicardial and endocardial borders of the left ventricle during end-systolic and end-diastolic phases in SAX. T2W-STIR and LGE images were qualitatively assessed for the presence of edema.

T1 and T2 mapping

The left ventricular myocardium was delineated by manually contouring the endocardial and epicardial borders, ensuring the exclusion of blood or epicardial fat. The inner trabeculated muscle layer was also omitted. These contours were copied to other images and adjusted accordingly. The final contours were transferred to a color map as illustrated in Figure 1. The myocardial region of interest (ROI) was semi-automatically segmented into a 16-segment bull's-eye plot following the American Heart Association (AHA) model: 6 basal, 6 mid-ventricular, and 4 apical segments [21]. The edematous myocardial segments were identified as regions within the left ventricle exhibiting hyperintensity on T2W STIR images and enhancement on late gadolinium images. The threshold used for signal intensity indicating myocardial edema was 2 standard deviations above the mean intensity of a reference region of interest (ROI) placed in remote unaffected myocardium (180° from the affected zone and lacks the visible evidence of infarction such as edema, enhancement, or wall motion abnormalities on cine images) [22, 23]. Microvascular obstruction (MVO) was characterized by the presence of a dark zone within an area of gadolinium enhancement. To quantify T1 and T2 values in regions of MVO, T1 and T2 map images were matched with the corresponding late gadolinium enhancement (LGE) images by slice position. Measurements were then conducted on the T1 and T2 maps within the regions of interest as determined by LGE [24]. In total, 320 segments were analyzed across the 20 patients and classified into three categories: normal segments, infarct segments without microvascular obstruction (MVO), and infarct segments with MVO. Results were averaged and compared for each segmental level (i.e. basal, mid-ventricular, and apical slices). Additionally, overall average T1 and T2 values were calculated for each segmental level.

Statistical analysis

Statistical analysis was conducted using the Statistical Package for the Social Sciences (SPSS) version 23. Categorical data are presented as numbers and percentages, while continuous variables are expressed as mean ± SD or median (interquartile range), as appropriate. Student's t-test and one-way analysis of variance (ANOVA), with Bonferroni's post-hoc test, were employed for comparing two and more than two normally distributed variables, respectively. All values are reported as mean ± SD and statistical significance was set at a p-value of less than 0.05.

Results

Study population

The age of the 20 enrolled patients ranged from 39 to 62 years, with a mean age of 51.50 ± 9.02 years. Among the patients, 13 were males and 7 were females. Regarding cardiovascular risk factors, 16 patients (80%) had hypertension, 12 patients (60%) had diabetes mellitus, 13 patients (65%) were smokers, and 11 patients (55%)

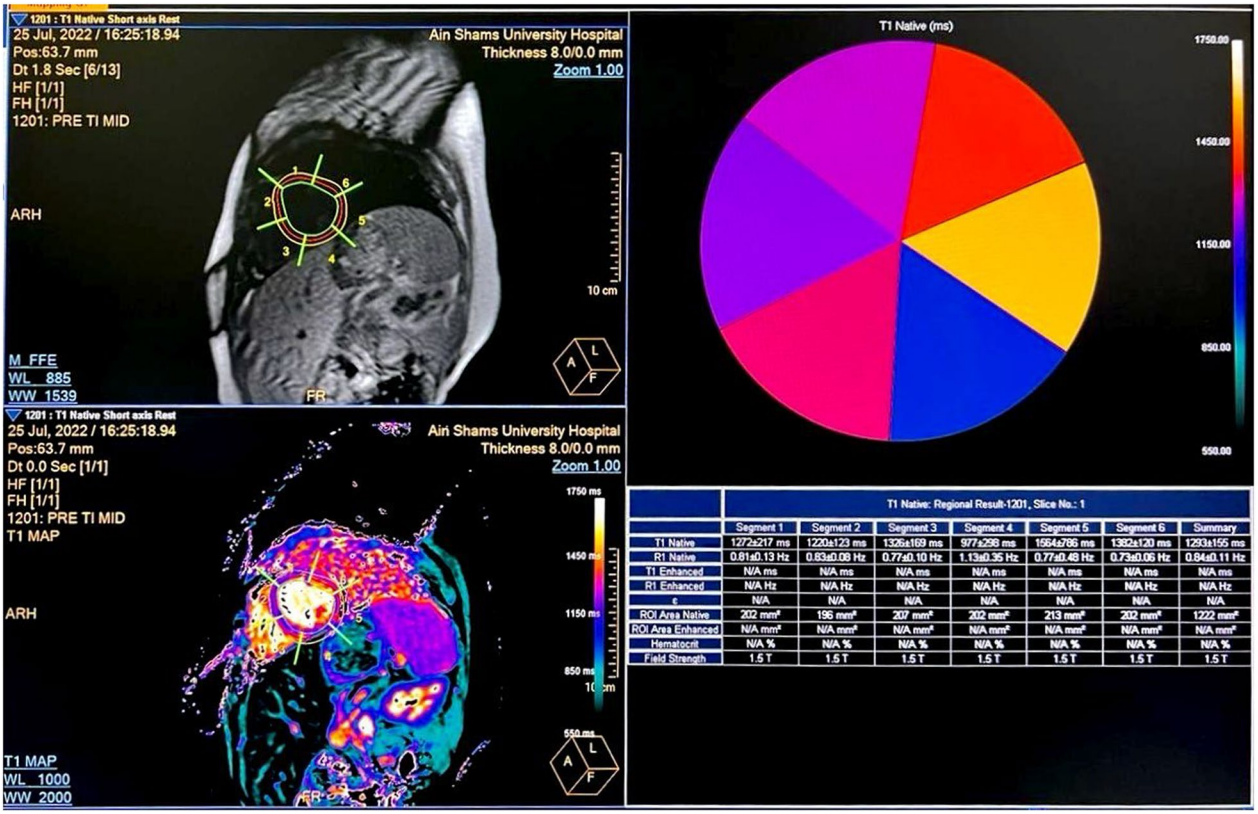

Fig. 1 Demonstration of contouring and semi-automatic segmentation of the left ventricular myocardium in the mid-ventricular slice of T1 map images. On the left side, segmentation according to the AHA 16-segment model is shown. The right side shows a table displaying the measured T1 values for each myocardial segment of that slice

had a positive family history of coronary artery disease in a first-degree relative. None of the patients had a history of any cardiac events before the current admission. The left anterior descending artery was the most affected, observed in 60% of patients, followed by the left circumflex artery (25%) and the right coronary artery (15%). The time from admission to CMR acquisition was 24–72 h.

CMR findings

Left ventricular function

All patients exhibited decreased overall left ventricular systolic function, with a mean left ventricular ejection fraction of 48% (range: 38–59%)

T1 and T2 mapping

Native T1 and T2 mapping images were able to identify myocardial edema and differentiate infarct from remote myocardium in 100% of the patients. The results of quantitative native T1 and T2 mapping are shown in Table 1. The average native T1 measured in infarct areas was 1115.38 ± 137.72 ms, 1161.25 ± 123.72 ms, and 1225.71 ± 134.05 ms in the basal, mid-ventricular, and apical segments, respectively. The average T2 measured in infarct areas was 59.88 ± 11.56 ms, 57.15 ± 12.52 ms, and 68.00 ± 10.17 in the same respective segments.

Table 1 Average native T1 values of infarct areas in basal, mid-ventricular, and apical segments

		T1	T2
Basal	Mean ± SD–ms	1115.38 ± 137.72	59.88 ± 11.56
	Range–ms	916–1378	48–85
Mid-ventricular	Mean ± SD–ms	1161.25 ± 123.72	57.15 ± 12.52
	Range–ms	971–1564	45–85
Apical	Mean ± SD–ms	1225.71 ± 134.05	68.00 ± 10.17
	Range–ms	900–1377	50–83

Effect of microvascular obstruction (MVO) on native T1 and T2 values

Overall, evidence of microvascular obstruction (MVO) was observed in 12 out of the 20 patients. As illustrated in Table 2, The average native T1 value measured in normal myocardium, infarct areas without microvascular obstruction (MVO), and infarct areas

Table 2 Average native T1 and T2 values in normal segments, infarct segments without MVO, and infarct segments with MVO

		Normal	Infarct without MVO	Infarct with MVO	Test value•	*P*-value	Sig.
T1-ms	Mean ± SD	1074.95 ± 92.86	1295.50 ± 87.65	1115.05 ± 64.70	221.493	0.000	HS
	Range	900–1226	1142–1564	1011–1200			
T2-ms	Mean ± SD	52.53 ± 6.26	74.63 ± 6.51	53.65 ± 3.56	467.669	0.000	HS
	Range	35–64	60–85	48–59			

	Post Hoc analysis by LSD		
	Normal vs. infarct without MVO	Normal vs. infarct with MVO	Infarct without MVO vs. infarct with MVO
T1	< 0.001	0.095	< 0.001
T2	< 0.001	0.427	< 0.001

P-value > 0.05: Non significant (NS); *P*-value < 0.05: Significant (S); *P*-value < 0.01: highly significant (HS)

*:Chi-square test; •: One Way ANOVA test

with MVO was 1074.95 ± 92.86 ms, 1295.50 ± 87.65 ms, and 1115.05 ± 64.70 ms, respectively, and the average T2 value measured in the same respective areas was 52.53 ± 6.26 ms, 74.63 ± 6.51 ms, and 53.65 ± 3.56 ms. Both native T1 and T2 values were significantly higher in infarct areas without MVO compared to normal myocardium and infarct areas with MVO ($p < 0.001$). However, no statistical significance was observed between native T1 and T2 values of normal myocardium, and infarct areas with MVO ($p = 0.095$ for T1 and $p = 0.427$ for T2). Table 3 presents average native T1 and T2 values after additional stratification based on the ventricular segmental levels (i.e. basal, mid-ventricular, and apical).Across all segmental levels, native T1 and T2 values were significantly higher in infarct areas without microvascular obstruction (MVO) compared to normal myocardium, and infarct areas with MVO ($p < 0.001$ for all segmental levels), and no statistical significance was observed between native T1 and T2 values of normal myocardium, and infarct areas with MVO for basal, mid-ventricular, and apical segmental ($p = 0.115$, $p = 0.255$, and $p = 0.956$ for T1; $p = 0.430$, $p = 0.148$, and $p = 0.861$ for T2, respectively).The average T1 and T2 mapping values in normal myocardium, infarct myocardium without MVO, and infarct myocardium with MVO, respectively across the basal, mid-ventricular, and apical segments are displayed on a clustered bar chart in Figures 2 and 3.

In this illustrative case from our study, a 52-year-old male presented with acute myocardial infarction (AMI) affecting the left circumflex artery (LCX) territory. Following admission, the patient underwent coronary angiography and percutaneous coronary intervention (P-PCI) in the culprit artery. Cardiac MRI was performed 36 h after admission, revealing a calculated ejection fraction of 51%. The CMR images are displayed in three short-axis (SAX) slices, namely basal, mid-ventricular, and apical, as shown in Table 4.

In another case, a 61-year-old male presented with an acute myocardial infarction (AMI) involving the left anterior descending (LAD) artery territory. The patient underwent coronary angiography followed by percutaneous coronary intervention (PCI) and stent placement in the affected artery. Cardiac MRI was performed 24 h after admission, revealing an ejection fraction (EF) of 48%. The CMR images are displayed in three short-axis (SAX) slices: basal, mid-ventricular, and apical, as detailed in Table 5.

Discussion

The key findings of our study are 1. Native T1 and T2 mapping accurately identified post-infarction myocardial edema in all patients. 2. The most important finding is that infarct myocardial segments can be quantitively differentiated from remote myocardium by their significantly higher native T1 and T2 values. 3. The average native T1 and T2 values of areas of microvascular obstruction were lower than those of the infarct myocardium and not significantly different from those of the remote myocardium.

In our study, native T1 and T2 mapping techniques successfully detected myocardial edema in 100% of the patients, consistent with previous research [7, 25–27]. In contrast, a study by Tessa et al. [14] reported lower rates of edema detection, possibly due to differences in imaging timing and patient selection. Our imaging was mostly conducted 1–3 days after admission, while Tessa et al. performed imaging within the first 24 h. Given the dynamic nature of myocardial edema in the first week after AMI, results may vary between early and later imaging acquisitions [28]. Additionally, our patients underwent imaging after coronary angiography, potentially

Table 3 Average T1 and T2 values in the normal segments, infarct segments without MVO, and infarct segments with MVO, stratified by LV segmental level (basal, mid-ventricular, and apical)

		Normal	Infarct without MVO	Infarct with MVO	Test value	*P*-value	Sig.
T1–msec							
Basal	Mean ± SD	1040.53 ± 94.08	1284.29 ± 59.16	1085.50 ± 78.53	100.677	0.000	HS
	Range	916–1201	1200–1378	1011–1160			
Mid	Mean ± SD	1046.50 ± 102.69	1285.33 ± 80.48	1050.00 ± 70.71	66.558	0.000	HS
	Range	900–1200	1142–1377	1000–1100			
Apical	Mean ± SD	1111.93 ± 75.85	1335.60 ± 122.87	1144.60 ± 27.00	57.983	0.000	HS
	Range	971–1226	1205–1564	1112–1200			
T2–msec							
Basal	Mean ± SD	53.07 ± 4.08	72.58 ± 6.89	52.00 ± 0.00	438.211	0.000	HS
	Range	48–60	60–83	52–52			
Mid	Mean ± SD	51.65 ± 7.95	76.60 ± 6.76	53.50 ± 3.54	107.084	0.000	HS
	Range	35–64	68–85	51–56			
Apical	Mean ± SD	54.33 ± 4.27	76.71 ± 4.33	55.30 ± 4.55	62.087	0.000	HS
	Range	50–60	70–85	48–59			

	Post Hoc analysis by LSD		
	Normal vs. abnormal without MVO	Normal vs. abnormal with MVO	Abnormal without MVO vs. abnormal with MVO
T1			
Basal	< 0.001	0.115	< 0.001
Mid	< 0.001	0.255	< 0.001
Apical	< 0.001	0.956	< 0.001
T2			
Basal	< 0.001	0.430	< 0.001
Mid	< 0.001	0.148	< 0.001
Apical	< 0.001	0.861	< 0.001

P-value > 0.05: Non significant (NS); *P*-value < 0.05: Significant (S); *P*-value < 0.01: highly significant (HS)

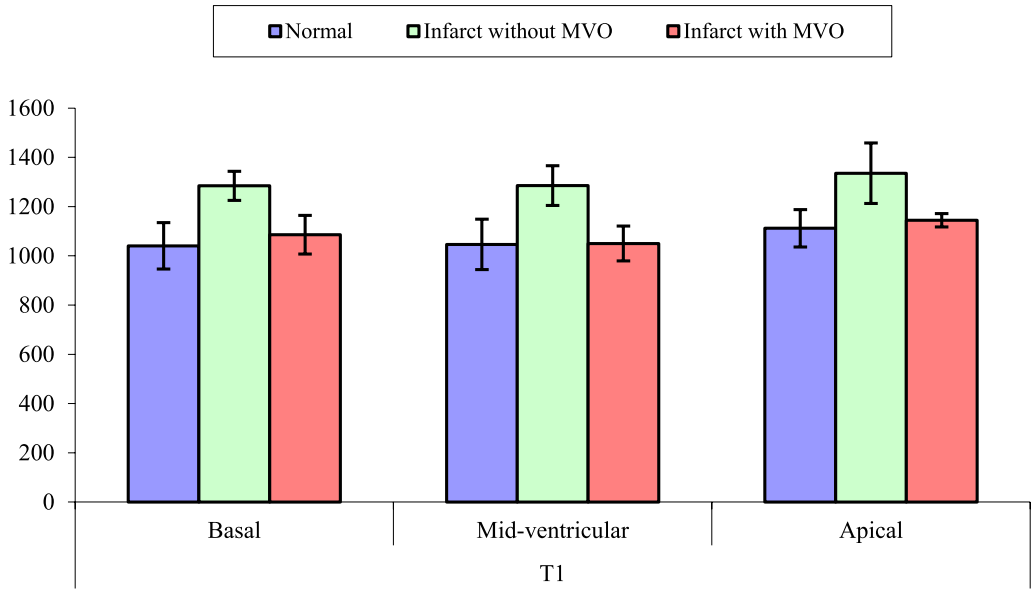

Fig. 2 Clustered bar chart displaying the average native T1 values in the basal, mid-ventricular, and apical segments in normal myocardium, infarct myocardium without MVO, and infarct myocardium with MVO, respectively

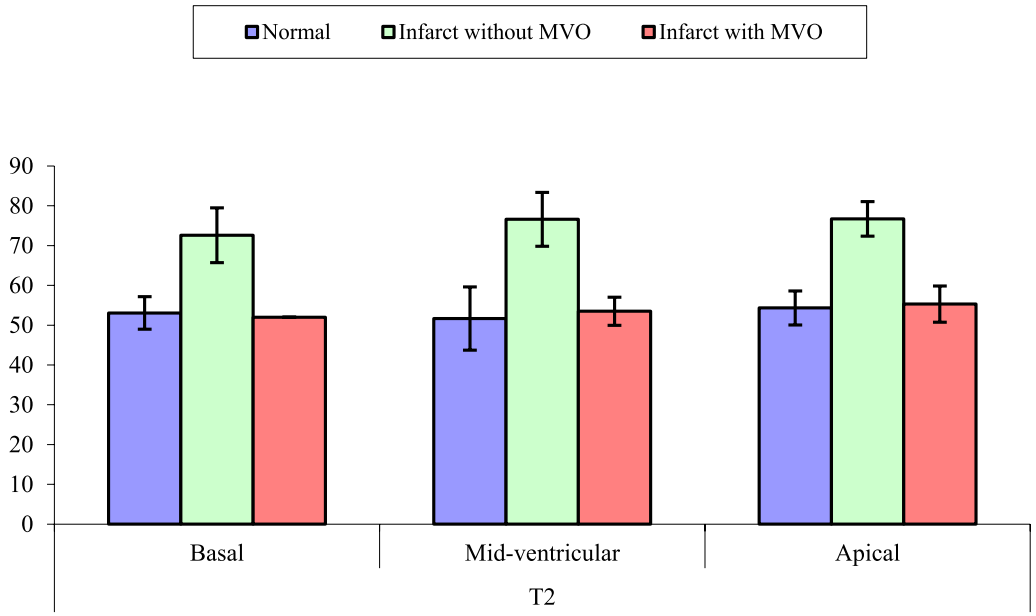

Fig. 3 Clustered bar chart displaying the average T2 values in the basal, midventricular, and apical segments in normal myocardium, infarct myocardium without MVO, and infarct myocardium with MVO, respectively

influencing edema severity. This distinction is important, as reperfusion injuries post-angiography could worsen myocardial edema [28]. Finally, unlike our study, Tessa et al. did not exclude patients with a history of myocardial infarction.

Quantification of native T1 and T2 maps

Early studies reported a linear correlation between myocardial free water content in myocardial infarction areas and T2 relaxation time prolongation [29]. However, discrepancies in native T1 and T2 relaxation times arise due to variations in field strength, CMR vendors, acquisition methods, and post-processing analysis, limiting their clinical utility and comparability between centers [30]. To address this, the Society for Cardiovascular Magnetic Resonance (SCMR) and the European Association of Cardiology Imaging (EACVI) recommend establishing local reference ranges of native T1 and T2 using standardized protocols [31]. Standardizing the methods for measuring T1 and T2 values will help improve data consistency and comparability. Determining cut-off values for native T1 and T2 to distinguish infarcted myocardium from healthy tissue has been extensively studied, with most studies indicating high accuracy using three [32] and two [26] standard deviations above the mean values of normal myocardium. In our study, the average T1 within the infarct zone was 1295.50 ± 87.65 ms, compared to 1074.95 ± 92.86 ms in remote myocardium, and the average T2 within the infarct zone was 74.63 ± 6.51 ms, compared to 52.53 ± 6.26 ms in remote myocardium. Similar values have been reported in other studies [14, 33, 34]. While the mean differences between infarcted and non-infarcted segments may seem relatively small in absolute terms (221 ms for native T1 and 22 ms for T2), there was little overlap in values between ischemic and non-ischemic regions due to a narrow distribution around the mean, aligning with findings from other studies [25, 35]. However, Montant et al. [36] reported no overlap of T2 values in infarct zones with those in remote myocardium or healthy controls.

Previous studies often reported native T1 and T2 values averaged across all myocardial segments or only for the mid-ventricular slice, which may overlook focal deviations in T1 and T2 values. While von Knobelsdorff-Brenkenhoff et al. [37] reported segment-specific values in normal patients, our study is, to our knowledge, the first to extend this analysis to both normal and post-infarction injured myocardium. Although our study didn't intend to directly compare native T1 and T2 values among basal, midventricular, and apical segments of normal and infarcted myocardium, we observed consistently higher native T1 and T2 values in apical segments compared to basal and mid-ventricular segments, in agreement with findings from other studies [11, 37, 38]. However, the underlying reasons for these differences remain uncertain. They could result from true biological variations between apical and more basal myocardial segments, motion artifacts in apical segments, or partial volume effects due to the curvature of the left ventricle, where blood signal might be included in the voxels of

Table 4 T2-weighted STIR (T2W-STIR), late gadolinium enhancement (LGE), T1 maps, and T2 maps images in basal, mid-ventricular, and apical segments

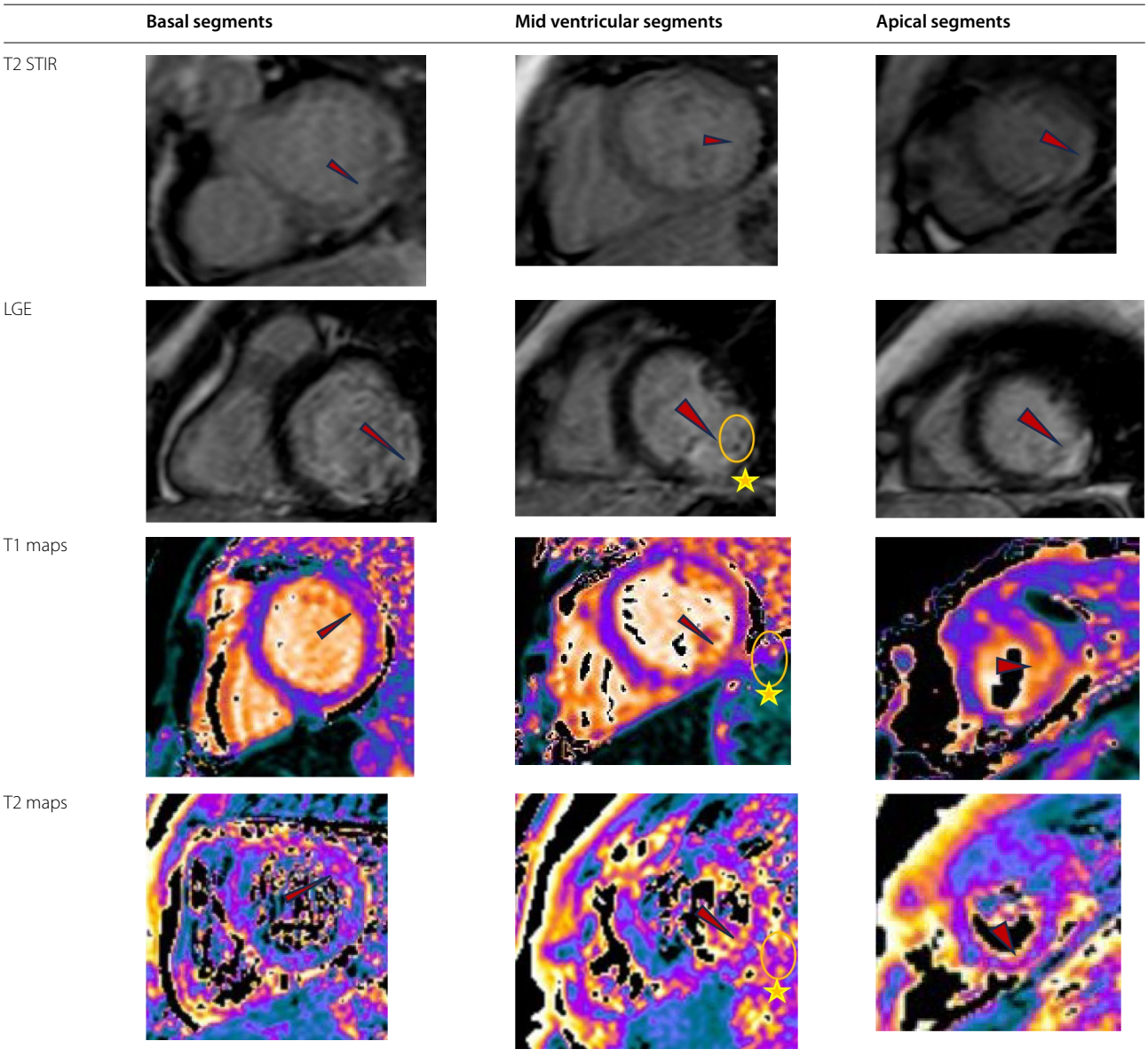

The red arrowheads indicate edematous myocardium within the infarct territory of the left circumflex artery (LCX). The T1 measured within the region of the infarct averaged 1300 ms compared to 920 ms in the remote myocardium. Similarly, the T2 measured within the region of the infarct was 79 ms compared to 55 ms in the remote myocardium. Additionally, the yellow star corresponds to two foci of microvascular obstruction (MVO) seen in LGE images and exhibits lower T1 values (934 ms) and T2 values (54 ms) than the surrounding edematous myocardium

apical segments [39]. Due to these uncertainties, some studies have chosen to exclude apical segments from their analyses [40, 41]. However, we attempted to mitigate this potential bias by meticulously contouring the myocardium to exclude the endocardial portion and the epicardial fat, and by using the highest possible isotropic spatial resolution. Nonetheless, further studies are warranted for further validation.

Effect of microvascular obstruction on native T1 and T2 values

Reperfusion therapy is the most effective strategy to preserve ischemic myocardium in acute myocardial infarction [33]. However, paradoxically it can also lead to reperfusion injury, characterized by microvascular obstruction (no-reflow) and intramyocardial hemorrhage. These complications are associated with poor

Table 5 T2-weighted STIR (T2W-STIR), late gadolinium enhancement (LGE), T1 maps, and T2 maps (displayed according to the 16-segment model) images in basal, mid-ventricular, and apical segments of Case (1)

	Basal segments	Mid ventricular segments	Apical segments
T2 STIR	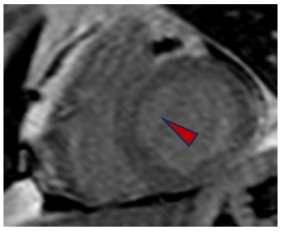	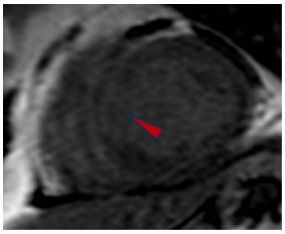	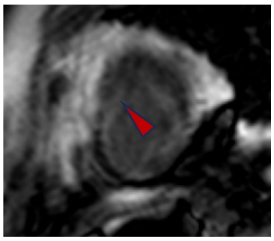
LGE	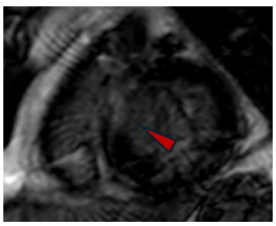	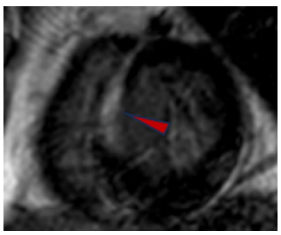	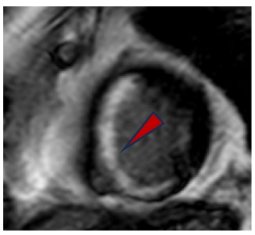
T1 maps	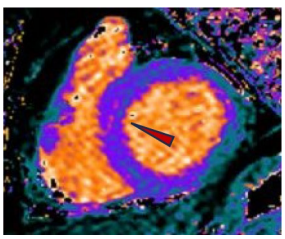	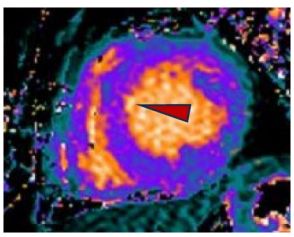	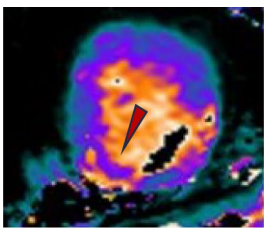
T2 maps	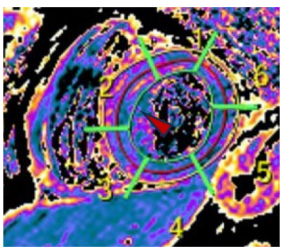	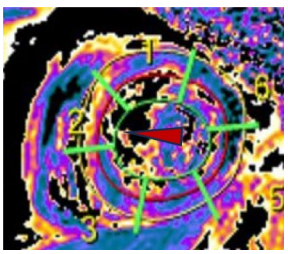	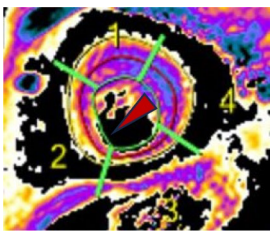

The red arrowheads indicate edematous myocardium within the infarct territory of the left anterior descending (LAD). The T1 measured within the region of the infarct averaged 1244 ms compared to 979 ms in the remote myocardium. Similarly, the T2 measured within the region of the infarct was 71 ms compared to 53 ms in the remote myocardium

functional recovery and adverse left ventricular remodeling [6, 12]. In a subset of patients within our study, we observed that the mean native T1 and T2 values of microvascular obstruction (MVO) were lower than those of infarct myocardium but not significantly different from those of remote myocardium. This observed "pseudo normalization" of T1 and T2 values within areas corresponding to MVO in late gadolinium enhancement (LGE) images is consistent with findings from previous studies [8, 12, 26, 42–44].

Edema is a key feature of ischemia-reperfusion injury, reflecting the inflammatory state of infarcted myocardial tissues [13]. Intramyocardial hemorrhage, a crucial histological finding of reperfusion injury, occurs when red blood cells extravasate through damaged endothelial walls after reperfusion [27]. This hemorrhage, often found in the infarct core, is closely associated with microvascular obstruction [25, 45]. Hemoglobin from extravasated red blood cells undergoes oxidative changes, producing paramagnetic substances like deoxyhemoglobin, methemoglobin, ferritin, and hemosiderin, which shorten native T1 and T2 values in areas of microvascular obstruction. Additionally, reduced water content in these areas further contributes to shorter relaxation times [27]. Microvascular obstruction (MVO) strongly correlates with increased infarct size in severe myocardial

infarctions and predicts impaired functional recovery, remodeling, and higher incidence of major adverse cardiac events (MACE) [44]. Also, Elevated T1 and T2 values are associated with more severe myocardial injury and less functional improvement [46]. However, interpreting native T1 and T2 measurements in recently reperfused acute myocardial infarction (AMI) can be complicated by magnetic susceptibility effects from hemorrhage in MVO areas [44]. For instance, Dall'armellina et al. explained the rise in native T1 values in severe myocardial infarctions but did not account for the presence or absence of MVO. Similarly, Carrick et al. [47] proposed that decreased native T1 values in the infarct core, associated with worse outcomes, were likely influenced by haemorrhage, yet they did not specifically analyse native T1 maps of the haemorrhagic MI core. Alkhalil et al. [48] acknowledged limitations in their study, where native T1 mapping analysis was solely based on the average of voxel derived T1 values, irrespective of the presence of MVO, potentially diminishing the ability to assess acute myocardial injury severity. However, they noted that this simplified approach avoided extensive post-processing. Furthermore, in these studies, native T1 and T2 relaxation times were averaged for the entire myocardium, potentially offsetting the lower values in the infarct cores of patients with MVO, as the MI border zone often exhibits higher T1 and T2 values [44]. Hence, it's crucial, aligning with other research, to acknowledge and document the presence of MVO and hemorrhage when analyzing myocardial segments post-infarction using native T1 and T2 mapping techniques [47]. This approach can improve the precision and reliability of native T1 and T2 measurements for evaluating myocardial injury severity and guiding clinical management decisions.

Study limitations

We acknowledge the following limitations: Firstly, the sample size was small, potentially affecting the correction for confounding factors influencing native T1 and T2 values, although the mapping consistently identified myocardial injury areas. Secondly, exclusion of high-risk patients might limit generalizability. Thirdly, the absence of gold standard for assessing myocardial edema/infarction challenged the study validation. Histological validation would have provided insight into the precise mechanisms underlying the observed changes in relaxation times. Fourthly, the measured T1 and T2 values are susceptible to various influences, including the sequence used, magnetic field strength, and CMR hardware and software parameters, among others. Careful consideration of these factors is essential during data interpretation [49]. The selection of the region of interest (ROI) for normal myocardium reference was drawn in remote myocardium. While some studies found no discrepancies in T2 values between the remote myocardium of acute myocardial infarction (AMI) patients and healthy controls [25], others reported elevated native T1 and T2 mapping values in AMI patients' remote myocardium [50, 51]. The underlying reasons for these discrepancies remain unclear, but proposed mechanisms include inflammatory responses triggered by coronary artery occlusion and reperfusion, leading to edema in the remote myocardium. Additionally, vasodilation of arteries supplying the remote myocardium in response to increased oxygen consumption might influence native T1 and T2 values [51]. Lastly, limitations related to left ventricular coverage in the study are acknowledged, with three 2D slices used. This approach aimed to balance comprehensive ventricular coverage with minimizing examination duration, especially in acute patients, following prior studies [7, 14, 25, 32, 52, 53]. Future advancements allowing full 3D coverage of the LV would improve sensitivity and reduce the risk of missing subtle pathological findings.

Conclusions

Parametric native T1 and T2 mapping techniques can detect and quantify myocardial edema arising from myocardial infarction. Moreover, they effectively assess microvascular obstruction resulting from revascularization injury. This knowledge holds significant clinical significance, profoundly impacting the diagnosis, guidance, and monitoring of myocardial infarction treatments.

Clinical implementation

Both native T1 imaging and T2 mapping yield comparable quantitative results for assessing injured myocardium following acute myocardial infarction, without requiring the use of contrast agents.

Abbreviations

ΔTE	Echo spacing
AHA	American Heart Association
AMI	Acute myocardial infarction
ANOVA	One-way analysis of variance
bSSFP	Balanced steady-state free precession
CMR	Cardiovascular magnetic resonance
EACVI	European Association of Cardiology Imaging
ED	Emergency Department
FA	Flip angle
FOV	Field of view
GraSE	Gradient spin-echo sequence
IMH	Intramyocardial hemorrhage
LCX	Left circumflex artery
LGE	Late gadolinium enhancement
LV	Left ventricular
LVEF	Left ventricular ejection fraction
MACE	Major adverse cardiac events
MOLLI	Modified look-locker inversion recovery
MR	Magnetic resonance
MRI	Magnetic resonance imaging
MVO	Microvascular obstruction

P-PCI	Primary percutaneous coronary intervention
PSIR	Phase-sensitive inversion-recovery gradient-echo T1 sequence
ROI	Region of interest
SAX	Stack of short-axis
SCMR	Society for Cardiovascular Magnetic Resonance
SENSE	Sensitivity encoding
SSFP	Steady-state free precession
T2W STIR	T2-weighted short tau inversion recovery
TE	Echo time
TR	Repetition time

Acknowledgements
The author thanks all the study participants for their patience and support.

Author contributions
MME: Recruited cases, collected and analyzed data, wrote the manuscript, performed necessary measurements and statistical analysis, and prepared figures and tables. BMR: Contributed to data analysis, reviewed literature, reviewed statistical analysis, and participated in manuscript editing. HGH: Reviewed the manuscript and provided input on statistical analysis. YMA: Assisted in case recruitment, data collection and analysis, reviewed literature, conducted statistical analysis, and participated in manuscript editing. ASI: Initiated the research idea, reviewed the manuscript, and provided input on statistical analysis. All authors have read and approved the final manuscript.

Funding
This study received no funding from any source.

Availability of data and materials
The datasets analyzed during the current study is available from the corresponding author on reasonable request.

Declarations

Ethics approval and consent to participate
This study received approval from the Research Ethics Committee of the Faculty of Medicine at Ain Shams University in Egypt in May 2020; Approval Reference Number: MD99/2020.

Consent for publication
Written informed consent was obtained from all patients included in this study for the publication of the data.

Competing interests
The authors declare no financial or non-financial competing interests.

Author details
[1]Diagnostic and Interventional Radiology Department, Faculty of Medicine, Ain Shams University, Cairo, Egypt. [2]Cardiology Department, Faculty of Medicine, Ain Shams University, Cairo, Egypt. [3]Faculty of Applied Health Sciences, Galala University, Suez, Egypt.

Received: 14 May 2024 Accepted: 19 August 2024
Published online: 02 September 2024

References

1. Dastidar AG, Baritussio A, Garate ED, Drobni Z, Biglino G, Singhal P, Milano EG, Angelini GD, Dorman S, Strange J, Johnson T, Bucciarelli-Ducci C (2019) Prognostic role of CMR and conventional risk factors in myocardial infarction with nonobstructed coronary arteries. JACC Cardiovasc Imaging 12(10):1973–1982
2. Perazzolo Marra M, Lima JA, Iliceto S (2011) MRI in acute myocardial infarction. Eur Heart J 32(3):284–293
3. Pedersen F, Butrymovich V, Kelbæk H, Wachtell K, Helqvist S, Kastrup J et al (2014) Short-and long-term cause of death in patients treated with primary PCI for STEMI. J Am Coll Cardiol 64(20):2101–2108
4. Kristensen SD, Laut KG, Fajadet J, Kaifoszova Z, Kala P, Di Mario C et al (2014) Reperfusion therapy for ST elevation acute myocardial infarction 2010/2011: current status in 37 ESC countries. Eur Heart J 35(29):1957–1970. https://doi.org/10.1093/eurheartj/eht529
5. Yellon DM, Hausenloy DJ (2007) Myocardial reperfusion injury. N Engl J Med 357(11):1121–1135
6. Fernández-Jiménez R, Sánchez-González J, Agüero J, García-Prieto J, López-Martín GJ, García-Ruiz JM et al (2015) Myocardial edema after ischemia/reperfusion is not stable and follows a bimodal pattern: imaging and histological tissue characterization. J Am Coll Cardiol 65(4):315–323
7. Layland J, Rauhalammi S, Lee MM, Ahmed N, Carberry J, Teng Yue May V et al (2017) Diagnostic accuracy of 3.0-T magnetic resonance T1 and T2 mapping and T2-weighted dark-blood imaging for the infarct-related coronary artery in non–ST-segment elevation myocardial infarction. J Am Heart Assoc 6(4):e004759
8. h-Ici DO, Jeuthe S, Al-Wakeel N, Berger F, Kuehne T, Kozerke S, Messroghli DR (2014) T1 mapping in ischaemic heart disease. Eur Heart J-Cardiovasc Imaging 15(6):597–602
9. Akber SF (2008) Water proton relaxation times of pathological tissues. Physiol Chem Phys Med NMR 40:1–42
10. Friedrich MG (2008) Tissue characterization of acute myocardial infarction and myocarditis by cardiac magnetic resonance. JACC Cardiovasc Imaging 1(5):652–662
11. Granitz M, Motloch LJ, Granitz C, Meissnitzer M, Hitzl W, Hergan K, Schlattau A (2019) Comparison of native myocardial T1 and T2 mapping at 1.5 T and 3T in healthy volunteers: reference values and clinical implications. Wien Klin Wochenschr 131:143–155
12. Germain P, El Ghannudi S, Jeung MY, Ohlmann P, Epailly E, Roy C, Gangi A (2014) Native T1 mapping of the heart-a pictorial review. Clin Med Insights Cardiol 8(Suppl 4):1–11. https://doi.org/10.4137/CMC.S19005
13. Ghugre NR, Pop M, Barry J, Connelly KA, Wright GA (2013) Quantitative magnetic resonance imaging can distinguish remodeling mechanisms after acute myocardial infarction based on the severity of ischemic insult. Magn Reson Med 70(4):1095–1105
14. Tessa C, Del Meglio J, Lilli A, Diciotti S, Salvatori L, Giannelli M et al (2018) T1 and T2 mapping in the identification of acute myocardial injury in patients with NSTEMI. Radiol Med 123:926–934. https://doi.org/10.1007/s11547-018-0931-2
15. Dabir D, Child N, Kalra A, Rogers T, Gebker R, Jabbour A et al (2014) Reference values for healthy human myocardium using a T1 mapping methodology: results from the International T1 Multicenter cardiovascular magnetic resonance study. J Cardiovasc Magn Reson 16(1):69. https://doi.org/10.1186/s12968-014-0069-x
16. Popescu IA, Werys K, Zhang Q, Puchta H, Hann E, Lukaschuk E, Ferreira VM, Piechnik SK (2021) Standardization of T1-mapping in cardiovascular magnetic resonance using clustered structuring for benchmarking normal ranges. Int J Cardiol 326:220–225. https://doi.org/10.1016/j.ijcard.2020.10.041
17. ESC Scientific Document Group, Collet JP, Thiele H, Barbato E, Barthélémy O, Bauersachs J, Bhatt DL et al (2021) 2020 ESC guidelines for the management of acute coronary syndromes in patients presenting without persistent ST-segment elevation. Eur Heart J 42(14):1289–1367. https://doi.org/10.1093/eurheartj/ehaa575
18. Radunski UK, Lund GK, Stehning C, Schnackenburg B, BohnenAdam SG et al (2014) CMR in patients with severe myocarditis: diagnostic value of quantitative tissue markers including extracellular volume imaging. JACC Cardiovasc Imaging 7(7):667–675. https://doi.org/10.1016/j.jcmg.2014.02.005
19. Ugander M, Oki AJ, Hsu LY, Kellman P, Greiser A, Aletras AH et al (2012) Extracellular volume imaging by magnetic resonance imaging provides insights into overt and sub-clinical myocardial pathology. Eur Heart J 33(10):1268–1278. https://doi.org/10.1093/eurheartj/ehr481
20. Tahir E, Sinn M, Bohnen S, Avanesov M, Säring D, Stehning C et al (2017) Acute versus chronic myocardial infarction: diagnostic accuracy of quantitative native T1 and T2 mapping versus assessment of edema on standard T2-weighted cardiovascular MR images for differentiation. Radiology 285(1):83–91. https://doi.org/10.1148/radiol.2017162338
21. American Heart Association Writing Group on Myocardial Segmentation and Registration for Cardiac Imaging, Cerqueira MD, Weissman NJ, Dilsizian V, Jacobs AK, Kaul S, Laskey WK et al (2002) Standardized

myocardial segmentation and nomenclature for tomographic imaging of the heart: a statement for healthcare professionals from the cardiac imaging committee of the council on clinical cardiology of the American Heart Association. Circulation 105(4):539–542. https://doi.org/10.1161/hc0402.102975
22. Kim RJ, Fieno DS, Parrish TB, Harris K, ChenSimonetti ELO et al (1999) Relationship of MRI delayed contrast enhancement to irreversible injury, infarct age, and contractile function. Circulation 100:1992–2002
23. Berry C, Kellman P, Mancini C, Chen MY, BandettiniLowrey WPT et al (2010) Magnetic resonance imaging delineates the ischemic area at risk and myocardial salvage in patients with acute myocardial infarction. Circ Cardiovasc Imaging 3:527–535
24. Bulluck H, Rosmini S, Abdel-Gadir A, Bhuva AN, Treibel TA, Fontana M et al (2017) Diagnostic performance of T1 and T2 mapping to detect intramyocardial hemorrhage in reperfused ST-segment elevation myocardial infarction (STEMI) patients. J Magn Reson Imaging 46(3):877–886. https://doi.org/10.1002/jmri.25638
25. Verhaert D, Thavendiranathan P, Giri S, Mihai G, Rajagopalan S, Simonetti OP, Raman SV (2011) Direct T2 quantification of myocardial edema in acute ischemic injury. JACC Cardiovasc Imaging 4(3):269–278. https://doi.org/10.1016/j.jcmg.2010.09.023
26. Dall'Armellina E, Piechnik SK, Ferreira VM, Le Si Q, Robson MD, Francis JM et al (2012) Cardiovascular magnetic resonance by non contrast T1-mapping allows assessment of severity of injury in acute myocardial infarction. J Cardiovasc Magn Reson 14(1):16. https://doi.org/10.1186/1532-429X-14-15
27. Shin JM, Choi EY, Park CH, Han K, Kim TH (2020) Quantitative T1 mapping for detecting microvascular obstruction in reperfused acute myocardial infarction: comparison with late gadolinium enhancement imaging. Korean J Radiol 21(8):978. https://doi.org/10.3348/kjr.2019.0736
28. Fernández-Jiménez R, Barreiro-Pérez M, Martin-García A, Sánchez-González J, Agüero J, Galán-Arriola C et al (2017) Dynamic edematous response of the human heart to myocardial infarction: implications for assessing myocardial area at risk and salvage. Circulation 136(14):1288–1300. https://doi.org/10.1161/CIRCULATIONAHA.116.025582
29. Higgins CB, Herfkens R, Lipton MJ, Sievers R, Sheldon P, Kaufman L, Crooks LE (1983) Nuclear magnetic resonance imaging of acute myocardial infarction in dogs: alterations in magnetic relaxation times. Am J Cardiol 52(1):184–188. https://doi.org/10.1016/0002-9149(83)90093-0
30. O'Brien AT, Gil KE, Varghese J, Simonetti OP, Zareba KM (2022) T2 mapping in myocardial disease: a comprehensive review. J Cardiovasc Magn Reson 24(1):33. https://doi.org/10.1186/s12968-022-00866-0
31. Snel GJ, van den Boomen M, Hernandez LM, Nguyen CT, Sosnovik DE, Velthuis BK et al (2020) Cardiovascular magnetic resonance native T2 and T2* quantitative values for cardiomyopathies and heart transplantations: a systematic review and meta-analysis. J Cardiovasc Magn Reson 22(1):34. https://doi.org/10.1186/s12968-020-00627-x
32. Messroghli DR, Moon JC, Ferreira VM, Grosse-Wortmann L, He T, Kellman P et al (2016) Clinical recommendations for cardiovascular magnetic resonance mapping of T1, T2, T2* and extracellular volume: a consensus statement by the Society for Cardiovascular Magnetic Resonance (SCMR) endorsed by the European Association for Cardiovascular Imaging (EACVI). J Cardiovasc Magn Reson 19(1):75. https://doi.org/10.1186/s12968-017-0389-8
33. Moulin K, Viallon M, Romero W, Chazot A, Mewton N, Isaaz K, Croisille P (2020) MRI of reperfused acute myocardial infarction edema: ADC quantification versus T1 and T2 mapping. Radiology 295(3):542–549
34. Tahir E, Sinn MR, Radunski UK, Säring D, Stehning C, Muellerleile K (2015) Serial native T1-and T2-mapping to quantitatively monitor resorption of myocardial edema following acute myocardial infarction. J Cardiovasc Magn Reson 17:1–2. https://doi.org/10.1186/1532-429X-17-S1-P101
35. Thavendiranathan P, Walls M, Giri S, Verhaert D, Rajagopalan S, Moore S et al (2012) Improved detection of myocardial involvement in acute inflammatory cardiomyopathies using T2 mapping. Circ Cardiovasc Imaging 5(1):102–110. https://doi.org/10.1161/CIRCIMAGING.111.967836
36. Montant P, Sigovan M, Revel D, Douek P (2015) MR imaging assessment of myocardial edema with T2 mapping. Diagn Interv Imaging 96(9):885–890. https://doi.org/10.1016/j.diii.2014.07.008
37. von Knobelsdorff-Brenkenhoff F, Prothmann M, Dieringer MA, Wassmuth R, Greiser A, Schwenke C et al (2013) Myocardial T 1 and T 2 mapping at 3 T: reference values, influencing factors and implications. J Cardiovasc Magn Reson 15:1–11. https://doi.org/10.1186/1532-429X-15-53
38. Markl M, Rustogi R, Galizia M, Goyal A, Collins J, Usman A et al (2013) Myocardial T2-mapping and velocity mapping: changes in regional left ventricular structure and function after heart transplantation. Magn Reson Med 70(2):517–526. https://doi.org/10.1002/mrm.24472
39. Böttcher B, Lorbeer R, Stöcklein S, Beller E, Lang CI, Weber MA, Meinel FG (2021) Global and regional test-retest reproducibility of native T1 and T2 mapping in cardiac magnetic resonance imaging. J Magn Reson Imaging 54(6):1763–1772. https://doi.org/10.1002/jmri.27755
40. Giri S, Chung YC, Merchant A, Mihai G, Rajagopalan S, Raman SV, Simonetti OP (2009) T2 quantification for improved detection of myocardial edema. J Cardiovasc Magn Reson 11(1):56. https://doi.org/10.1186/1532-429X-11-56
41. Wong TC, Piehler K, Meier CG, Testa SM, Klock AM, Aneizi AA et al (2012) Association between extracellular matrix expansion quantified by cardiovascular magnetic resonance and short-term mortality. Circulation 126(10):1206–1216. https://doi.org/10.1161/CIRCULATIONAHA.111.089409
42. Azarisman SM, Carbone A, Shirazi M, Bradley J, Teo KS, Worthley MI, Worthley SG (2016) Characterisation of myocardial injury via T1 mapping in early reperfused myocardial infarction and its relationship with global and regional diastolic dysfunction. Heart Lung Circ 25(11):1094–1106. https://doi.org/10.1016/j.hlc.2016.03.011
43. Biesbroek PS, Amier RP, Teunissen PF, Hofman MB, Robbers LF, van de Ven PM et al (2017) Changes in remote myocardial tissue after acute myocardial infarction and its relation to cardiac remodeling: a CMR T1 mapping study. PLoS ONE 12(6):e0180115. https://doi.org/10.1371/journal.pone.0180115
44. Robbers LF, Nijveldt R, Beek AM, Teunissen PF, Hollander MR, Biesbroek PS et al (2018) The influence of microvascular injury on native T1 and T2* relaxation values after acute myocardial infarction: implications for non-contrast-enhanced infarct assessment. Eur Radiol 28:824–832. https://doi.org/10.1007/s00330-017-5010-x
45. Beek AM, Nijveldt R, van Rossum AC (2010) Intramyocardial hemorrhage and microvascular obstruction after primary percutaneous coronary intervention. Int J Cardiovasc Imaging 26:49–55. https://doi.org/10.1007/s10554-009-9499-1
46. Dall'Armellina E, Ferreira VM, Kharbanda RK, Prendergast B, Piechnik SK, Robson MD et al (2013) Diagnostic value of pre-contrast T1 mapping in acute and chronic myocardial infarction. JACC Cardiovasc Imaging 6(6):739–742
47. Carrick D, Haig C, Rauhalammi S, Ahmed N, Mordi I, McEntegart M (2016) Prognostic significance of infarct core pathology revealed by quantitative non-contrast in comparison with contrast cardiac magnetic resonance imaging in reperfused ST-elevation myocardial infarction survivors. Eur Heart J 37(13):1044–1059. https://doi.org/10.1093/eurheartj/ehv372
48. Alkhalil M, Borlotti A, De Maria GL, Wolfrum M, DawkinsFahrni SG (2020) Hyper-acute cardiovascular magnetic resonance T1 mapping predicts infarct characteristics in patients with ST elevation myocardial infarction. J Cardiovasc Magn Reson 22(1):3. https://doi.org/10.1186/s12968-019-0593-9
49. Moon JC, Messroghli DR, Kellman P, Piechnik SK, RobsonUgander MDM (2013) Myocardial T1 mapping and extracellular volume quantification: a Society for Cardiovascular Magnetic Resonance (SCMR) and CMR Working Group of the European Society of Cardiology consensus statement. J Cardiovasc Magn Reson 15(1):92. https://doi.org/10.1186/1532-429X-15-92
50. Chan W, Duffy SJ, White DA, Gao XM, Du XJ, Ellims AH et al (2012) Acute left ventricular remodeling following myocardial infarction: coupling of regional healing with remote extracellular matrix expansion. JACC Cardiovasc Imaging 5(9):884–893. https://doi.org/10.1016/j.jcmg.2012.03.015
51. Reinstadler SJ, Stiermaier T, Liebetrau J, Fuernau G, Eitel C, de Waha S et al (2018) Prognostic significance of remote myocardium alterations assessed by quantitative noncontrast T1 mapping in ST-segment

elevation myocardial infarction. JACC Cardiovasc Imaging 11(3):411–419. https://doi.org/10.1016/j.jcmg.2017.03.015
52. McAlindon EJ, Pufulete M, Harris JM, Lawton CB, Moon JC, Manghat N (2015) Measurement of myocardium at risk with cardiovascular MR: comparison of techniques for edema imaging. Radiology 275(1):61–70. https://doi.org/10.1148/radiol.14131980
53. Raman SV, Simonetti OP, Winner MW, Dickerson JA, He X, Mazzaferri EL, Ambrosio G (2010) Cardiac magnetic resonance with edema imaging identifies myocardium at risk and predicts worse outcome in patients with non–ST-segment elevation acute coronary syndrome. J Am Coll Cardiol 55(22):2480–2488. https://doi.org/10.1016/j.jacc.2010.01.047

Publisher's Note